MICROSTRUCTURAL, PHYSICAL AND MECHANICAL PROPERTIES OF AERATED CONCRETE CONTAINING FLY ASH UNDER HIGH TEMPERATURE AND PRESSURE

ILHAMI DEMIR[1], OZER SEVIM[1 *], GOKHAN OZEL[2], ORHAN DOGAN[1]
[1]*Department of Civil Engineering, Kırıkkale University, Kırıkkale 71451, Turkey*
[2]*Graduate School of Natural and Applied Science, Kırıkkale University, Kırıkkale 71451, Turkey*

This study analyzed the effects of the use of fly ash as a replacement for the quartz sand on the compressive strength, dry density, moisture content and thermal conductivity of the aerated concrete. Based on the production of Class G2/04 aerated concrete, a commercially available wall construction element, aerated concrete samples were produced using the fly ash as a replacement for the silica sand (quartz sand) at additive ratios of 5%, 10%, 15%, 20%, and 25%. After steam curing the samples for 4 hours at 60 ºC, they were cured in an autoclave for 6.5 hours at 180 ºC under 11 bar pressures. As a result, the samples showed an increase in their dry density directly proportional to the fly ash addition ratio; and the highest dry density was found in the aerated concrete with 25% fly ash content. It was further observed that the moisture content increases as the fly ash addition ratio increases. Compressive strength was reduced with the fly ash addition. Thermal conductivity was found to be reduced up to fly ash addition ratio of 10%, however, it was then increased again up to fly ash addition of 25%. 25% fly ash replacement ratio is recommended in this study in terms of thermal conductivity, dry density, which are the most important properties of aerated concrete. Higher levels of fly ash replacement with sand can be actualized which can further enhance to the utilization of fly ash, raise awareness regarding waste minimization and reduce the overall costs of aerated concrete mixtures.

Keywords: *Aerated concrete, fly ash, compressive strength, dry density, moisture content, thermal conductivity*

1. Introduction

Autoclaved aerated concrete (AAC) is made of fine silica-based materials, porosity inducing materials, and binders such as cement and/or lime combined with water. Raw material is mixed, and the mixture is taken into molds where it will swell and create the paste. After this step, the paste is cut in desired size and cured in autoclave under high-pressure steam conditions [1-5]. J. A. Eriksson has taken the most important step in aerated concrete production and his method patented under the name of Durox in 1925 was started to be used in production in Switzerland [6]. Although the method did not attract much interest until the 50s, starting from this decade both European nations and others started to adopt this method [7]. Today, there is a research interest in the use of fly ash, as a waste material, in aerated concrete production. There are a number of thermal power stations operating in Turkey, Afsin-Elbistan, Catalagzı, Cayırhan, Kangal, Kemerkoy, Orhaneli, Seyitomer, Soma, Tuncbilek, Yatagan and Yenikoy, to name some of them. A significant amount of fly ash is produced in these plants operating in Turkey [8]. Globally, it can be repurposed only 25% of the fly ash produced in the world. Nations such as Germany, the Netherlands and Belgium use more than 95% of the fly ash produced, while the UK uses approximately 50% [8,9]. Therefore, the usage of fly ash in Turkey is increasing with each passing day.

Literature contains a number of studies on the use of fly ash in aerated concrete production. Drochytka and Helanova [10] tested the physical and mechanical properties and microstructure of aerated concrete samples containing fly ash under the effects of liquefaction and high temperature after being stored for 2 years under laboratory conditions. Song et al. [11] analyzed the effects of Ca/Si ratio on aerated concrete with two different types of fly ash. It was found that Ca/Si ratio had a significant impact on AAC hydrates and pore structure. Hausera et al. [12] explored the changes in the strength of conventional aerated concrete with fly ash content when replaced with lime sulphate. AAC with lime sulphate mixtures resulted in the highest compressive strengths. Walczak et al. [13] stated the contribution of the use of industrial waste to the environmental conservation and evaluated the production of concrete with fly ash at a density of 350 kg/m^3. Holt et al. [14] stated that fly ash reacts with lime as it has pozzolanic properties, which results in new bonds to reinforce the microstructure. Narayanan et al. [15] explored the structure of hydration products, the impact of fly

* Autor corespondent/*Corresponding author*,
E-mail: ozersevim@kku.edu.tr

ash addition on the pore structure, and transition zone in the hollow matrix interface and found that differences in the mixture ratios (sand to fly ash ratio) and the curing method used (steam curing/autoclave curing) have a significant effect on the microstructural properties of the aerated concrete. The authors suggested that aerated concretes with sand and fly ash content vary extensively in time due to their changing hydration levels and that although only cement is hydrated initially, this is followed by slow hydration of the fly ash. Kunhanandan Nambiar et al. [16] found that additive of sand with fly ash in aerated concrete resulted in increased strength. The authors noted that samples produced using cement and fly ash offered a relatively higher water absorption ratio when compared to cement and sand mixtures. Literature interest in usage of waste materials and fibers in relation to aerated concrete continues to grow in the recent years [17-21].

As shown in research of the previous studies, fly ash was tested both as an additive for cement at specific ratios and as a total replacement to quartzite. Nevertheless, the test samples are most commonly treated with low autoclave pressures. In this study, it has been replaced quartzite, the main material, with fly ash at specific ratios and used autoclave curing at high temperature and high pressure. In this study, based on the production of G2/04 (compressive strength, 2 MPa, and density, 400 kg/m^3) class aerated concrete, a commercially available wall construction element, aerated concrete samples were produced using the fly ash as a replacement for quartzite at additive ratios of 5%, 10%, 15%, 20%, and 25% and their compressive strength, dry density, moisture content, and thermal conductivity values were investigated.

2. Materials and methods

2.1.Materials

<u>Quartzite</u>

Quartzite used in this study was obtained from the Kırsehir-Boztepe quarry operated by AKG Aerated Concrete. For the production of aerated concrete, quartz sand is required to be of a certain fineness and the silica content is high. In addition, the clay content should be low. Chemical analysis of the material is given in Table 1.

<u>Fly Ash</u>

As a by-product of lignite coal burning, fly ash used in this study was obtained from Çatalagzı Thermal Power Station. The reason behind the preference of this specific fly ash was that it complies with the chemical component limits as reported in EN 197-1, ASTM C618 standards and that it has a high SiO_2 content [22,23]. Chemical analysis of fly ash was performed using XRF device, and chemical and physical properties of fly ash are listed in Table 2. The total amount of SiO_2+Al_2O_3+Fe_2O_3 in the fly ash was 82.62% of the material. According to ASTM C618, it is

Table 1

Chemical analysis of quartzite

Chemical properties	Quartzite
SiO_2	89.72
Al_2O_3	2.09
Fe_2O_3	1.12
K_2O	1.05
CaO	1.14
MgO	0.18
SO_3	-
Na_2O	0.12

Table 2

Chemical and physical properties of fly ash and cement

Chemical properties	Fly ash	Cement
SiO_2	43.25	20.13
Al_2O_3	20.72	5.07
Fe_2O_3	18.65	3.52
CaO	3.55	62.04
MgO	2.31	2.34
SO_3	1.48	2.60
Na_2O	1.01	0.61
K_2O	8.20	0.77
Loss of ignition	1.07	2.36
Physical properties		
Specific surface area(cm^2/g)	2820	3759
Specific gravity (unitless)	2.45	3.17

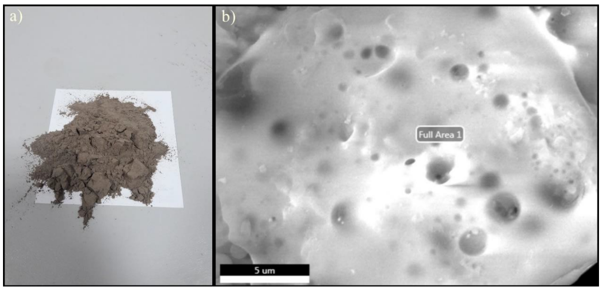

Fig. 1 - F Class fly ash (a) optical image and (b) SEM image.

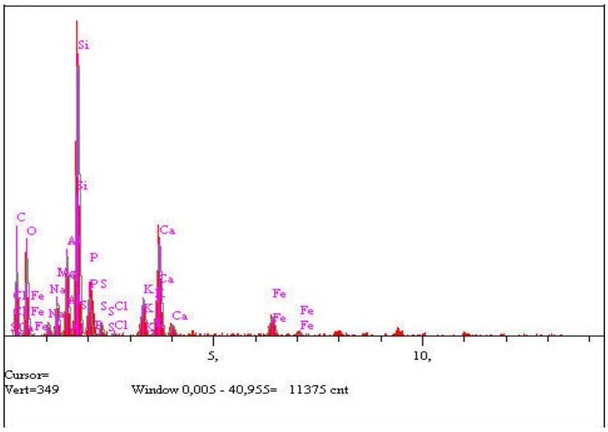

Fig. 2 - EDX analysis of fly ash.

classified under Class F (low lime content) as its SiO_2+Al_2O_3+Fe_2O_3 content was 82.61% and its CaO content was lower than 10% [22,23]. Therefore, it can be said that the material is glassy and contains low amounts of crystalline phases. Crystalline phases consist of quartz, mullite, biotite (mica group minerals) and hematite. Optical and SEM image of fly ash are given in Fig. 1 and EDX analysis of fly ash is given in Fig. 2.

Cement

Cement used in the mixtures was CEM I 42.5 R (ordinary portland cement). It was observed that the physical and chemical properties of the cement comply with the limits stated in the EN 197-1 and EN 197- 2 standards [23,24]. Chemical and physical properties of ordinary portland cement are listed in Table 2. The Specific surface area of cement used that is 3759 cm^2/g. Optical and SEM image of CEM I 42.5 R ordinary portland cement are given in Fig. 3.

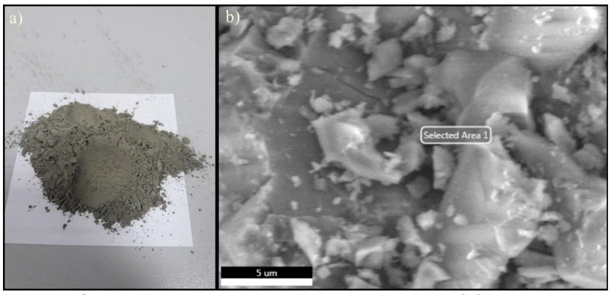

Fig. 3 - CEM I 42.5 R ordinary portland cement (a) optical image and (b) SEM image.

Lime

Lime was obtained from Akyuz Lime. According to the chemical analysis of lime, CaO ratio was 94.75% and the loss on ignition was 3.21%.

Gypsum

Gypsum was obtained from Kılıcoglu Gypsum. CaO ratio was 29.50%, SO_3 ratio was 42.09% relative moisture content was 18.96%, and the loss on ignition was 2.04%.

Aluminum Powder

Aluminum powder used in this study was obtained from AKG Kırıkkale Aerated Concrete Manufacturing Plant. Aluminum/mixture water ratio was taken approximately 1:3.75 to obtain aluminum in suspension during aerated concrete production.

2.2.Methods

Based on the production of G2/04 class aerated concrete, a commercially available wall construction element, aerated concrete samples were produced using the fly ash obtained from Catalagzı Thermal Power Station as a replacement for the quartz sand at additive ratio of 5%, 10%, 15%, 20%, and 25%. The reason behind this selection of additive ratios was that it was attempted to obtain a minimum ratio of total SiO_2 between 75-78%. Table 3 shows the SiO_2 ratio of the main material used in the experiments.

Table 4 shows the mix ratios of all the materials used in the experiment. An experimental mold of 15×25×20 cm^3 (length × wide × high) size was used in this study.

In the preparation of the mixture, firstly; fly ash, quartz sand and gypsum were taken into a container and a third of the mixture water was added; after mixing cement and lime in a separate container, this mixture was added on the first mixture and the remaining two-thirds was added and the mixture was stirred until it is homogeneous. Mixed with a specific amount of

Table 3

SiO_2 ratio of the main material used in the experiments.

Additive ratio (%)	Quartzite (kg)	Fly Ash (kg)	Total Raw Material (kg)	SiO_2 Ratio (%)
Control	168	0	168	89.72
5	160	8	168	85.25
10	151	17	168	82.89
15	143	25	168	80.79
20	134	34	168	78.43
25	126	42	168	76.33

Table 4

Material used in the experiment and mix ratios for 1 m^3

Ingredient (kg)	Control	FA5	FA10	FA15	FA20	FA25
Quartzite	168	160	151	143	134	126
Fly ash	0	8	17	25	34	42
Cement	91	91	91	91	91	91
Lime	31	31	31	31	31	31
Gypsum	29	29	29	29	29	29
Water	262	262	262	262	262	262
Aluminum	0.55	0.55	0.55	0.55	0.55	0.55

water to obtain a paste, aluminum suspension was then added to the mixture and it was stirred. Aerated concrete mortar in a viscous form was then taken into the greased molds. The reason behind aluminum suspension being added to the mixture at the end is that it initiates a reaction at the moment it is introduced in the mixture. A reaction between aluminum and lime takes place and the aerated concrete mix starts to expand [25]. The chemical reaction of aerated concrete is described below [26].

$$2Al + 3Ca(OH)_2 + 6H_2O \longrightarrow$$
$$\longrightarrow 3CaO{\cdot}Al_2O_3{\cdot}6H_2 + 3H_2$$

Hydrogen gas produced with this reaction leads to expansion and pore formation. Crystals of tobermorite, one of the most common in aerated concrete, forms as a result of the reactions taking place under high pressure and high temperature in autoclave [26]. After samples were subjected to steam curing for 4 hours at 60 ºC, they were taken out of molds. Samples placed in the steam curing line rapidly started to expand and settling. A partially hardened aerated concrete paste was obtained having expanded due to the bubbles created by the hydrogen produces as a result of the reactions taking place in about 30 mins. Samples were then placed in the autoclave and were subjected to steam curing for about 6.5 to 7 hours at 180 °C under 11 bar pressure using saturated steam. After the steam curing, samples were light, porous and resistant to high pressure.

2.2.1. Testing of microstructural, physical and mechanical properties

Compressive strength, specific weight, moisture content of the produced aerated concrete samples was defined, and they were subjected to thermal conductivity tests and microstructural analysis were analyzed using scanning electron microscope (SEM).

<u>Compressive Strength</u>

Experimental samples were prepared in accordance with EN 679 standard and were subjected to compressive strength tests. For the compressive strength test, a total number of 6 samples, one from each group, with the size of 10×10×10 cm^3 was used. Compressive strength test was performed using a computer-assisted testing device of the AKG Kırıkkale Aerated Concrete Labs [27]. Aerated concrete samples were collected from autoclave, and size of 10×10×10 cm^3 for compressive strength test. In the compressive strength test, after the test samples were rested at 60 °C stove for a day, they were removed from the stove and waited for about 2 h to cool to ambient temperature. During the test, the load was applied perpendicular to the expansion direction. The compressive load was then increased at a rate of 0.05 $N/mm^2/s$. The highest compressive load of experimental sample could carry was read at 0.01 N/mm^2 (MPa) accuracy. This method was then replicated for other samples and the compressive strengths were obtained.

<u>Dry Density</u>

Experimental samples were prepared in accordance with EN 678 standard and were subjected to dry density tests. Experimental samples were kept in a drying oven at 105 ºC until their masses are stable and then their weight was recorded using a precision scale. Similarly, their sizes were measured and recorded with caliper [28].

<u>Moisture Content</u>

Experimental samples were prepared in accordance with EN 772-10 standard and were subjected to moisture content tests. Samples, before being subjected to drying process, were weighed to define their moist weight and their densities were calculated [29]. This was then followed by drying the samples in a ventilated drying oven at 105°C ± 5°C temperature until their masses are stable and their densities were calculated.

<u>Thermal Conductivity Test</u>

Thermal conductivity test was performed accordance to ISO 8301 standard. "Lasercomp Fox 314" thermal conductivity testing device in Mechanical Engineering Labs of the Engineering Department of Kırıkkale University, was used to measure thermal conductivity coefficients (λ) of the samples [30]. The samples subjected to thermal conductivity test were 300×300×35 mm^3 (length × wide × high) in size.

<u>Microstructural Analysis</u>

Jeol JSM 5600 30kV Scanning Electron Microscope found in Scientific and Technological Research Labs of Kırıkkale University, was used to take SEM images of the experimental samples. Firstly, the samples were coated with gold to prepare their surface for SEM and then SEM images were taken using the Scanning Electron Microscope.

3.Results and discussion

Dry density, compressive strength, thermal conductivity and moisture content tests were conducted on the references sample (Control) Class G2/04 aerated concrete, and samples with fly ash additive ratios of 5%, 10%, 15%, 20% and 25%. The results are also given Table 5.

Table 5

Physical properties and compressive strengths of the AACs

Additive ratio (%)	Compressive Strength (MPa)	Dry Density (kg/m³)	Moisture Content (%)	Thermal Conductivity (W/m·K)
Control	2.47	406.0	8.37	0.105
5	2.28	409.7	8.70	0.095
10	2.02	413.5	10.45	0.092
15	1.93	410.3	12.10	0.097
20	1.86	411.2	13.68	0.098
25	1.85	407.4	13.79	0.102

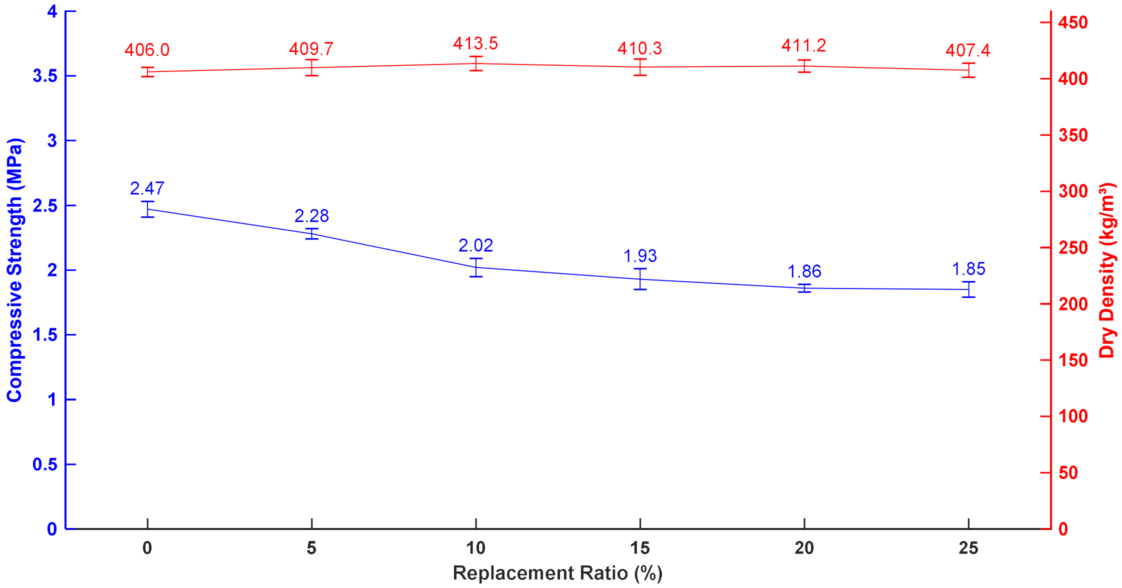

Fig. 4 - Compressive strength and dry density diagram of the AACs.

3.1.Compressive strength and dry density properties

As shown in Fig. 4 and Table 5, compressive strength of control sample was found to be 2.47 MPa while the same was found in the range between 2.28 MPa and 1.85 MPa for the aerated concrete samples having fly ash. The highest value of the sample was obtained with 5% fly ash content and this finding was about 8% lower than reference sample. The lowest compressive strength, 1.85 MPa, was obtained from aerated concrete with 25% fly ash content and this finding was about 25% lower than reference sample. Fly ash containing samples offered compressive strengths consistently lower than reference sample. This decrease in the compressive strength was sharp up to the sample with 10% fly ash content while it was slower in aerated concrete samples with fly ash replacement ratios of between 10% and 20%. However, a slight increase in the compressive strength was reported for the ratio higher than 20%.

It was found that compressive strength was reduced with the fly ash addition. It is believed that this effect can be accounted for by the reduced C- S-H crystal formation due to the reduced amount of SiO_2 available in the concrete because of increasing fly ash content as shown in Table 4.It is also believed that the fact that fly ash absorbs some portion of the water content disturbs the water to cement ratio which can be a factor in this effect [11,15,31]. For aerated concrete, it is sufficient to have enough compressive strength to carry its own weight [20,21]. The compressive strength of aerated concrete samples with 25% fly ash is sufficient to carry its own weight.

As shown in Fig. 4 and Table 5, dry density of control sample was found to be 406 kg/m³ while the same was found in the range between 413.5 kg/m³ and 407.4 kg/m³ for the aerated concrete samples with fly ash. All dry density results are similar. According to the results, all the samples were classified under 450 density class as reported in EN 12602 [1]. It was observed that dry density increases with fly ash replacement ratio. And this is raised by the fact that the use of fly ash restrains pore formation in aerated concrete leading to a structure weak in porosity. The fact that the SiO_2 content of fly ash is lower than that of quartz restrains the expansion of aerated concrete leading to decreasing void structure [11,32]. The compressive strength of aerated concrete samples with 25% fly ash is enough to carry its own weight, hence it is recommended to use 25% fly ash

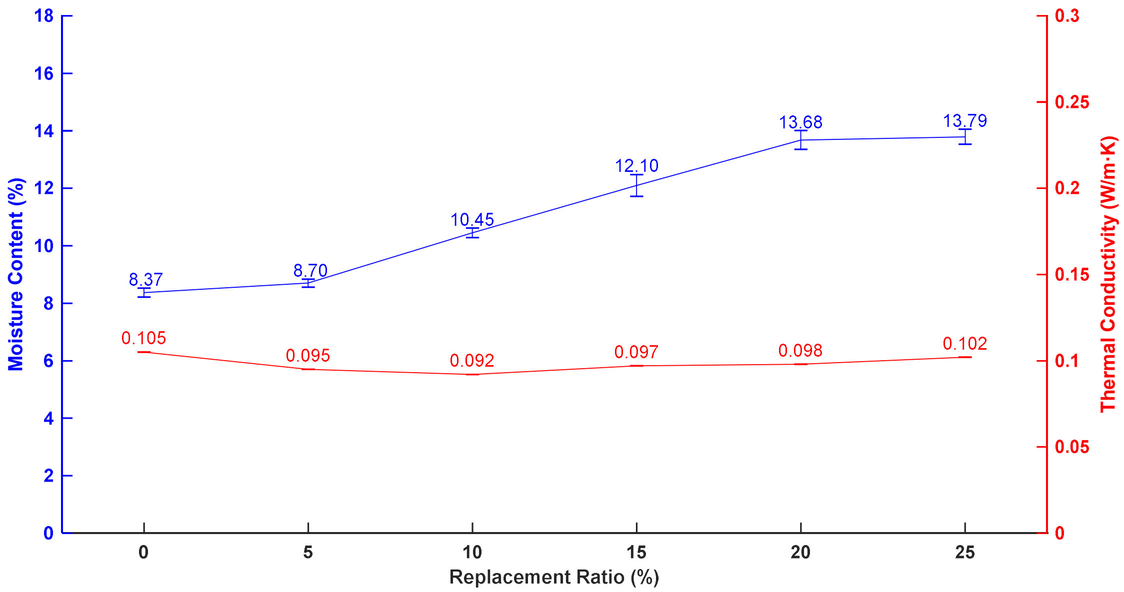

Fig. 5 - Moisture content and thermal conductivity diagram of the AACs.

additive in terms of compressive strength and dry density.

3.2. Moisture content and Thermal conductivity properties

As shown in Fig. 5, moisture content of the experimental samples is calculated in accordance with EN 772-10 standard [29]. Generally, it was observed that the moisture content increases as the fly ash additive ratio increases. The increase in filled pores with increasing fly ash additive ratio and increasing specific weight made it harder for the samples to dehumidify [10]. As the compressive strength decrease, void structure increase, hence moisture content increase.

As shown in Fig. 5 and Table 5, thermal conductivity coefficient of control sample, was found to be 0.105 W/(m·K) while the same was found in the range between 0.092 and 0.102 W/(m·K) for the aerated concrete samples with fly ash content. It was found that fly ash additive reduces the thermal conductivity coefficient up to the ratio of 10% obtaining the lowest coefficient 0.092 W/(m·K), and this value was 13% lower than reference sample. Moreover, 15-25% additive ratios lead to increased thermal conductivity coefficient. A lower thermal coefficient was obtained using aerated concrete samples having 25% fly ash than the control aerated samples without fly ash, therefore 25% fly ash additive is recommended in terms of moisture content and thermal conductivity.

3.3. Microstructural properties

SEM images of the samples were taken using Jeol JSM5600 30kV Scanning Electron Microscope found in Scientific and Technological Research Lab of Kırıkkale University, and the microstructural properties of the aerated concrete samples evaluated using difference fly ash additive ratio. In Scanning Electron Microscopy (SEM), the image is transferred to a screen of a cathode ray tube by passing the effects of elastic and non-elastic collisions between electron and sample atoms during scanning of the electron beam, which is accelerated by high voltage and focuses on the sample surface.

In order to see the effectiveness of fly ash, microstructural analysis of samples with control, 5%, 10%, and 20% fly ash additive rate were carried out on 28-day aerated concrete samples.

Fig. 6(a) is 35× magnification image of the control sample, and shows that pores are formed independently with sizes ranging between 1 and 1.5 mm. At 2000× magnification image given in Figure 6(b) shows a porous structure and some C-S-H (tobermorite) crystals. In the EDX analysis of the control sample is shown in Fig. 7, its chemical structure was found to be 47.211% CaO, 38.944% SiO_2, 4.748% P_2O_5, 3.130% Al_2O_3, 2.876% SO_3, 1.042% MgO.

Fig. 8(a) is a 35× magnification image of having 10% fly ash content and shows that pores are unstable and formed independently. Fig. 8(b) shows 1000× magnification image of having 10% fly ash content including pores in sizes ranging between 0 and 10 μm and some C-S-H (tobermorite) crystals In the EDX analysis of the sample having 10% fly ash is shown in Fig. 9, its chemical structure was found to be 46.638% CaO, 36.018% SiO_2, 8.016% P_2O_5, 3.355% Al_2O_3, 2.736% SO_3, 0.82% MgO.

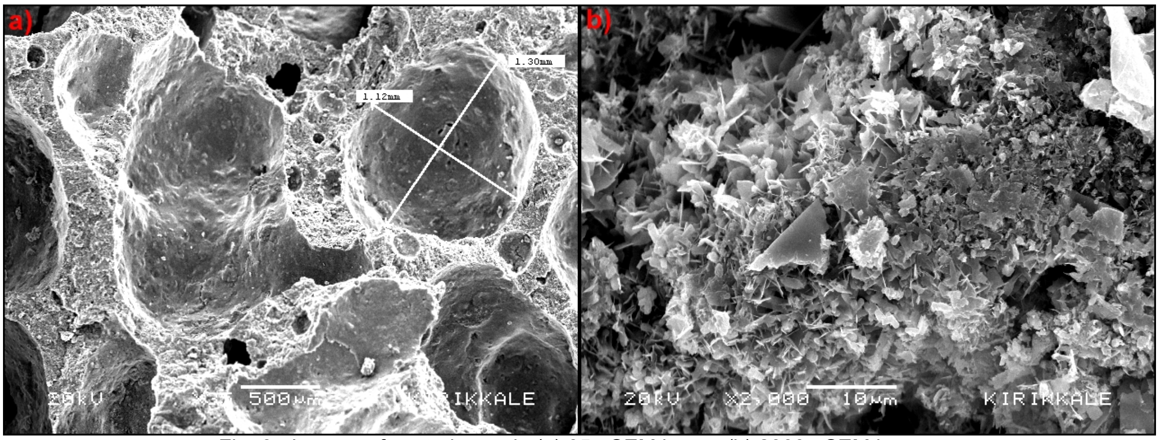

Fig. 6 - Images of control sample (a) 35× SEM image (b) 2000× SEM image.

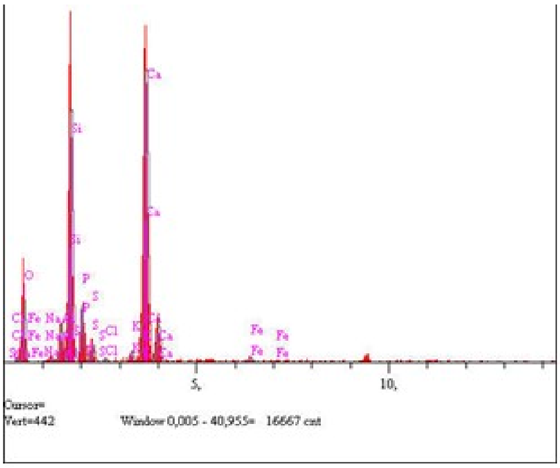

Component	Type	Mole Conc.	Conc.	
CO2	Calc	0,000	0,000	wt.%
Na2O	Calc	0,250	0,239	wt.%
MgO	Calc	1,042	0,648	wt.%
Al2O3	Calc	3,130	4,924	wt.%
SiO2	Calc	38,944	36,103	wt.%
P2O5	Calc	4,748	10,398	wt.%
SO3	Calc	2,876	3,552	wt.%
Cl2O	Calc	0,263	0,352	wt.%
K2O	Calc	0,844	1,227	wt.%
CaO	Calc	47,211	40,849	wt.%
Fe2O3	Calc	0,693	1,708	wt.%
		100,000	100,000	wt.%

Fig. 7 - EDX analysis of control sample.

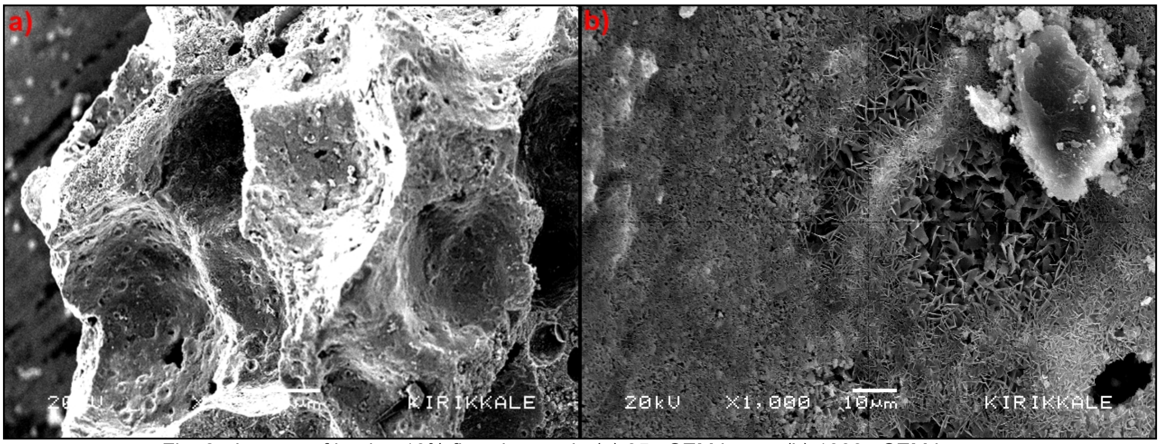

Fig. 8 - Images of having 10% fly ash sample (a) 35× SEM image (b) 1000× SEM image.

Fig. 10(a) is 35× magnification image of having 20% fly ash content and shows that pores are formed independently with sizes ranging between 1 mm and 2 mm. Fig. 10(b) shows 5000× magnification image of having 20% fly ash content contains C-S-H crystals resembling spongy. C-S-H gels are found extensively in sizes ranging between 0 and 5 µm. Also, pores can be seen prominently. In the EDX analysis of the sample having 20% fly ash is shown in Fig. 11, it was determined that 44.693% CaO, 39.804% SiO_2, 6.693% P_2O_5, 3.900% Al_2O_3, 2.094% SO_3, 0.396% MgO.

Figures 7, 9 and 11 show that SiO_2 and CaO are main component as we expect. However, EDS analysis consists of components that do not have a major effect due to impurity materials and elemental analysis. These may also be due to the fact that the place is not flat during EDS analysis, the X-ray is reflected differently and gives different mineral results. P_2O_5 is present in the raw material of cement manufacture [33]. The influence of P_2O_5 or calcium phosphate on the formation, stability and properties of calcium silicates in Portland clinker has already been investigated by

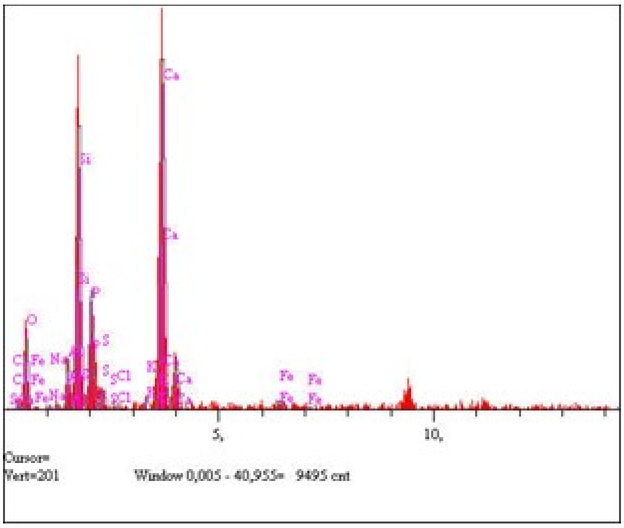

Component	Type	Mole Conc.	Conc.	
C O2	Calc	0,000	0,000	wt.%
Na2O	Calc	0,467	0,426	wt.%
MgO	Calc	0,820	0,486	wt.%
Al2O3	Calc	3,355	5,034	wt.%
SiO2	Calc	36,018	31,853	wt.%
P2O5	Calc	8,016	16,747	wt.%
SO3	Calc	2,736	3,225	wt.%
Cl2O	Calc	0,198	0,253	wt.%
K2O	Calc	0,662	0,918	wt.%
CaO	Calc	46,638	38,494	wt.%
Fe2O3	Calc	1,090	2,562	wt.%
		100,000	100,000	wt.%

Fig. 9 - EDX analysis of samples having 10% fly ash.

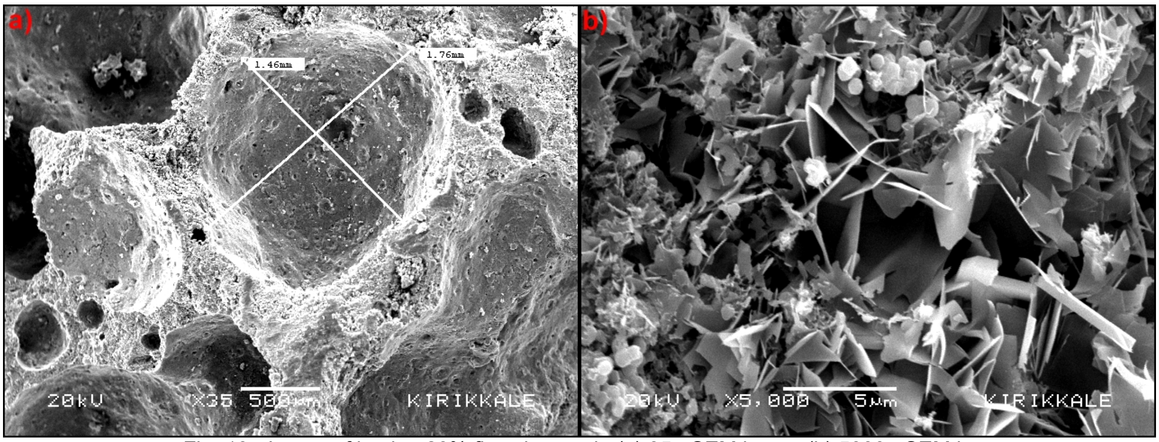

Fig. 10 - Image of having 20% fly ash sample (a) 35× SEM image (b) 5000× SEM image.

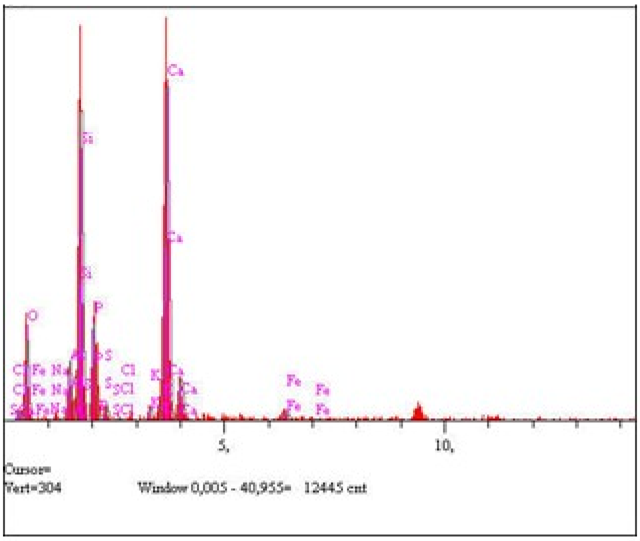

Component	Type	Mole Conc.	Conc.	
C O2	Calc	0,000	0,000	wt.%
Na2O	Calc	0,157	0,145	wt.%
MgO	Calc	0,396	0,237	wt.%
Al2O3	Calc	3,900	5,905	wt.%
SiO2	Calc	39,804	35,521	wt.%
P2O5	Calc	6,693	14,110	wt.%
SO3	Calc	2,094	2,490	wt.%
Cl2O	Calc	0,180	0,232	wt.%
K2O	Calc	0,831	1,162	wt.%
CaO	Calc	44,693	37,224	wt.%
Fe2O3	Calc	1,254	2,974	wt.%
		100,000	100,000	wt.%

Fig. 11 - EDX analysis of samples having 20% fly ash.

many authors [33-36]. It was demonstrated that phosphate takes an active part in the reactions during clinker burning process and shifts the stability limits of individual phases with formation of solid solutions [37].

As a result, a closer look into the microstructures of control, and having 10%, 20% fly ash additive showed that the pores are formed independently at all additive ratios. C-S-H (tobermorite) gels are formed in every additive ratio and these are shown in Figs. 6-11. As seen in the microstructure images, increasing additive ratio reduces the porosity, however, the pore diameter increases. The decrease in compressive strength can be explained by the increase in the pore diameter [38-40].

4.Conclusions

The following results are obtained from this study for reference sample Class G2/04 aerated concrete, and samples with fly ash additive ratios of 5%, 10%, 15%, 20% and 25%.

- There were no significant differences were found in terms of sample density, and all of the samples remained in the same density class (450 density) as in accordance with EN 12602 standard.
- For aerated concrete, it is sufficient to have enough compressive strength to carry its own weight. The compressive strength of aerated concrete samples with 25% fly ash is enough to carry its own weight.
- Fly ash was replaced by cement in previous studies. It has been shown that quartz sand can be replaced by this study.
- A lower thermal coefficient was obtained using aerated concrete samples having 25% fly ash than the control aerated samples without fly ash, therefore 25% fly ash additive is recommended in terms of moisture content and thermal conductivity.
- It is thought that the replacement of quartz sand with fly ash in aerated concrete has an adverse impact on its compressive strength, however, this effect can be neutralized with the use of fly ash with higher SiO_2 content.
- When seen in the microstructure images, increasing additive ratio reduces the porosity, however, the pore diameter increases. The decrease in compressive strength can be explained by the increase in the pore diameter

In conclusion, analysis of the compressive strength, dry density, and moisture content of the aerated concrete samples produced with the replacement of quartz sand with fly ash additive ratios of 5%, 10%, 15%, 20%, and 25% showed that it is possible to use fly ash as a replacement for quartz up to the additive ratio of 25%. The use of 25% additive ratio is recommended in this study when considering the only thermal conductivity which is a very important feature for autoclaved aerated concrete. Higher levels of fly ash replacement with sand can be actualized which can further enhance to utilization of fly ash, raise awareness regarding waste minimization and reduce the overall costs of aerated concrete mixtures.

REFERENCES

[1] TS EN 12602, Prefabricated reinforced components of autoclaved aerated concrete, Turkish Standards Institution, Ankara, 2016 (in Turkish).

[2] X. Li, Z. Liu, Y. Lv, L. Cai, D. Jiang, W. Jiang, S. Jian, Utilization of municipal solid waste incineration bottom ash in autoclaved aerated concrete, Construction and Building Materials, 2018, **178**, 175-182.

[3] G. Lin, C.L. Wang, C.Y. Qiao, H.L. Cui, L. Chen, S. Yu, Preparation and properties of autoclaved aerated concrete containing lead-zinc tailings, Romanian Journal of Materials, 2016, **46**(3), 334.

[4] X.Y. Liang, D.X. Yuan, J. Li, C.L. Wang, X.R. Lin, N. Chang, Preparation and phase characteristics of autoclaved aerated concrete using iron ore tailings, Revista Romana de Materiale, 2018, **48**(3), 381-387.

[5] C.L. Wang, W. Ni, S.Q. Zhang, S. Wang, G.S. Gai, W.K. Wang, Preparation and properties of autoclaved aerated concrete using coal gangue and iron ore tailings, Construction and Building Materials, 2016, **104**, 109-115.

[6] J.A. Eriksson, Device for ejecting paste and cream from collapsible tubes, U.S. Patent 1,546,221, July 14, 1925.

[7] N. Narayanan, K. Ramamurthy, Structure and properties of aerated concrete: a review, Cement and Concrete composites, 2000, **22**(5), 321-329.

[8] S. Uyanık, M. Topeli, The opportunities and challenges of fly Ash in Turkey, Report, September 2014.

[9] H. Aruntaş, Uçucu Küllerin Inşaat Sektöründe Kullanim Potansiyeli, Gazi Üniversitesi Mühendislik-Mimarlık Fakültesi Dergisi, 2006 **21**(1), 193-203 (in Turkish).

[10] R. Drochytka, E. Helanová, Development of microstructure of the fly ash aerated concrete in time, Procedia Engineering, 2015, **108**, 624-631.

[11] Y. Song, C. Guo, J. Qian, T. Ding, Effect of the Ca-to-Si ratio on the properties of autoclaved aerated concrete containing coal fly ash from circulating fluidized bed combustion boiler, Construction and Building Materials, 2015, **83**, 136-142.

[12] A. Hauser, U. Eggenberger, Mumenthaler, T, Fly ash from cellulose industry as secondary raw material in autoclaved aerated concrete. Cement and Concrete Research, 1999, **29**(3), 297-302.

[13] Walczak, P., Szymański, P. Różycka, A, Autoclaved aerated concrete based on fly ash in density 350kg/m3 as an environmentally friendly material for energy-efficient constructions. Procedia Engineering, 2015, **122**, 39-46.

[14] E. Holt, P. Raivio, Use of gasification residues in aerated autoclaved concrete, Cement and Concrete Research, 2005, **35**(4), 796-802.

[15] N. Narayanan, K. Ramamurthy, Microstructural investigations on aerated concrete, Cement and Concrete Research, 2000, **30**(3), 457-464.

[16] E.K. Nambiar, K. Ramamurthy, Influence of filler type on the properties of foam concrete, Cement and Concrete Composites, 2006, **28**(5), 475-480.

[17] R. Xu, T. He, Y. Da, Y. Liu, J. Li, C. Chen, Utilizing wood fiber produced with wood waste to reinforce autoclaved aerated concrete, Construction and Building Materials, 2019, **208**, 242-249.

[18] T. He, R. Xu, Y. Da, R. Yang, C. Chen, Y. Liu, Experimental study of high-performance autoclaved aerated concrete produced with recycled wood fibre and rubber powder, Journal of Cleaner Production, 2019, **234**, 559-567.

[19] B. Yuan, C. Straub, S. Segers, Q.L. Yu, H.J.H. Brouwers, Sodium carbonate activated slag as cement replacement in autoclaved aerated concrete, Ceramics International, 2017, **43**(8), 6039-6047.

[20] Z.O. Pehlivanlı, I. Uzun, Z.P. Yücel, Z.P. I. Demir, The effect of different fiber reinforcement on the thermal and mechanical properties of autoclaved aerated concrete, Construction and Building Materials, 2016, **112**, 325-330.

[21] Z.O. Pehlivanlı, I. Uzun, I. Demir, Mechanical and microstructural features of autoclaved aerated concrete reinforced with autoclaved polypropylene, carbon, basalt and glass fiber, Construction and Building Materials, 2015, **96**, 428-433.
[22] ASTM C618-19, Standard specification for coal fly ash and raw or calcined natural pozzolan for use in concrete, West Conshohocken, PA, ASTM International, 2019.
[23] TS EN 197-1, Cement-Part 1: Composition, specifications and conformity criteria for common cements, Turkish Standard Institution, Ankara, Turkey, 2012.
[24] TS EN 197-2, Cement-Part 2: Conformity evaluation. Turkish Standard Institution, Ankara, Turkey, 2014.
[25] J. Schreiner, J. Daniel, E. Dominique, G. N. Friedlinde, N. Juergen, S. Volkmann, New analytical possibilities for monitoring the phase development during the production of autoclaved aerated concrete, Cement and Concrete Research, 2018, **107**, 247-252.
[26] N. Y. Mostafa, Influence of air-cooled slag on physicochemical properties of autoclaved aerated concrete, Cement and Concrete Research 2005, **35**(7), 1349-1357.
[27] TS EN 679, Determination of the compressive strength of autoclaved aerated concrete, Turkish Standards Institution, Ankara, Turkey, 2008 (in Turkish).
[28] TS EN 678, Determination of the dry density of autoclaved aerated concrete, Turkish Standards Institution, Ankara, Turkey, 1995 (in Turkish).
[29] TS EN 772-10, Methods of test for masonary units- Part 10: Determination of moisture content of calcium silicate and autoclaved aerated concrete units, Turkish Standards Institution, Ankara, Turkey, 2000 (in Turkish).
[30] TS ISO 8301, Thermal insulation – Determination of steady - state thermal resistance and related properties - Heat flow meter apparatus, Turkish Standards Institute, Ankara, Turkey, 2002 (in Turkish).
[31] Y. Xia, Y. Yan, Z. Hu, Utilization of circulating fluidized bed fly ash in preparing non-autoclaved aerated concrete production, Construction and Building Materials, 2013, **47**, 1461-1467.
[32] K. Kunchariyakun, S. Asavapisit, S. Sinyoung, Influence of partial sand replacement by black rice husk ash and bagasse ash on properties of autoclaved aerated concrete under different temperatures and times, Construction and Building Materials, 2018, **173**, 220-227.
[33] R.W. Nurse, The effect of phosphate on the constitution and hardening of Portland cement, Journal of applied chemistry, 1952, **2**(12), 708-716.
[34] W. Gutt, High temperature phase equilibria in the system 2CaO·SiO2–3CaO·P2O5– CaO, Nature, 1963, **197**, 142–149.
[35] W. Gutt, Manufacture of Portland cement from phosphatic raw materials, 15th ICCC, Tokyo, Japan, 1968, 93–105.
[36] L. Halicz, Y. Nathan, L. Ben-Dor, The influence of P2O5 on clinker reactions, Cement Concrete and Research, 1984, **14**(1), 11–18.
[37] S. Puntke, Auswirkungen des Phosphateintrages in Drehofenanlagen der Zementindustrie auf Klinkermineralogie und Zementeigenschaften, Dissertation, TU Clausthal, 2004.
[38] I. Demir, S. Güzelkücük, O. Sevim, Effects of sulfate on cement mortar with hybrid pozzolan substitution, Engineering Science and Technology, an International Journal, 2018, **21**(3), 275-283.
[39] O. Sevim, I. Demir, Physical and permeability properties of cementitious mortars having fly ash with optimized particle size distribution, Cement and Concrete Composites, 2019, **96,** 266-273.
[40] O. Sevim, I.Demir, Optimization of fly ash particle size distribution for cementitious systems with high compactness, Construction and Building Materials, 2019, **195**, 104-114.

****